Geophys. J. Int. (2008) **175,** 449–461 doi: 10.1111/j.1365-246X.2008.03821.x

Mineral magnetic properties of artificial samples systematically mixed from haematite and magnetite

Ute Frank and Norbert R. Nowaczyk

GeoForschungsZentrum Potsdam, Section 3.3. *Climate Dynamics and Sedimentats, Telegrafenberg,* D-14473 *Potsdam, Germany.*
E-mail: ufrank@gfz-potsdam.de

Accepted 2008 April 10. Received 2008 April 7; in original form 2007 September 21

SUMMARY

Detailed rock magnetic investigations were carried out on a set of samples with defined ratios of haematite and magnetite. The measured parameters provide a reference for interpreting common rock magnetic parameters in investigations of sediments. The contribution of haematite to the magnetic fraction must exceed 95 wt-% of the magnetic fraction when mixed with magnetite in order to visibly influence grain size and coercitivity indicative magnetic parameters. Coercivity of remanence (B_{CR}) and coercive force (B_C) do not change in the same way with increasing haematite content, which results in a peak B_{CR}/B_C value at around 99.5 wt-% haematite. Variations in haematite content can be ignored when interpreting most rock magnetic parameters, especially grain size indicative parameters for samples where haematite contents range from 0 to 98 wt-%. The S-ratio is still the most sensitive parameter for estimating the relative amount of haematite in magnetite/haematite mixtures. A combination of S-ratio, the saturation isothermal remanent magnetization divided by the low field magnetic susceptibility (SIRM/κ_{LF}) and B_{CR} is the most effective way to identify haematite in natural samples. Our results agree with literature data and fill the gap between results obtained either from pure magnetite or haematite with comparable grain sizes.

Key words: Rock and mineral magnetism.

INTRODUCTION

Haematite is a common magnetic mineral in sediments and rocks. Its presence is often inferred from rock magnetic measurements including isothermal remanent magnetization (IRM) acquisition curves, the S-ratio and the 'hard' IRM (HIRM). Examples are given by Liu *et al.* (2003), Geiss *et al.* (2003), Larrasoaña *et al.* (2003), Wang *et al.* (2004), Inoue *et al*. (2004), Kumar *et al*. (2005) and Demory *et al.* (2005). Although the magnetic characteristics of pure haematite have been well studied (e.g. Dankers 1981; Dekkers & Linsen 1989; Robert*s et al.* 2006), relatively little is known about the varying contributions from haematite to the magnetic characteristics of bulk sediments in which (Ti-) magnetite is the dominant magnetic mineral. Bloemendal *et al.* (1992) and Roberts *et al.* (1995) analysed samples with variable, but well defined, haematite/magnetite concentrations and with different magnetite grain sizes. FORC (first-order reversal curve) diagrams on haematite/magnetite mixtures have been measured by Muxworthy *et al.* (2005) and Carvallo *et al.* (2006). Based on known parameters for haematite, theoretical predictions were also made (Roberts *et al.* 1995), but these are to sparse to enable interpretation of rock magnetic results from natural samples, let alone the innumerable possible combinations within variations in grain size and concentrations. In addition, the linear additivity of remanences and coercitivity dependent parameters samples mixed from different magnetic minerals, as presented here, could not be demonstrated (Roberts *et al*. 1995; Carter-Stiglitz *et al*. 2001; Carvallo *et al*. 2006), in contrast to samples mixed from magnetite with different grain sizes (Lees 1997; Muxworthy *et al*. 2005; Carvallo *et al*. 2006). Thus, rock magnetic parameters predicted for magnetic mineral mixtures will suffer from large errors (Roberts *et al*. 1995). The intention of this study is to give a visual impression of how the standard rock magnetic parameters, especially the anhysteretic remanent magnetization (ARM) and the grain size indicative rock magnetic parameter ratios, are influenced by varying haematite contents and laboratory procedures. The results presented here were obtained from a series of experiments on artificially mixed samples with known contributions from technically produced magnetite and haematite with constant grain sizes but with varying magnetite/haematite ratios.

METHODS

The studied haematite and magnetite powders were produced by Alfa Aesar® GmbH & Co KG (Karlsruhe, Germany), with a specified purity of 99.945 per cent for Fe_2O_3 and 99.997 per cent for Fe_3O_4. The grain sizes of the Fe_2O_3 and Fe_3O_4 powders are <5 and 2 μm, respectively. Samples were prepared by mixing weighed quantities of haematite and magnetite powders, together with Al_2O_3 powder as a non-magnetic matrix, and epoxy resin for mechanical stabilization. The mixtures were stirred with a glass stick for

Table 1. Rock magnetic analyses carried out on samples with different magnetite/haematite mixing ratios.

Analyses	Instrument	Remarks	Number of samples
Measurement of low-field magnetic susceptibility (κ_{LF})	AGICO Kappabridge MFKL1	Operating frequency 875 Hz	46 samples (6 cm^3)
Imparting of an anhysteretic remanent magnetization (ARM)	2G Enterprises 600 single-axis demagnetizer including an ARM-coil (max. static field 1 mT)	Produced along positive *z*-axis static field: 0.5 mT, peak AF amplitude: 100 mT	46 samples (6 cm^3)
Measurement and demagnetization of ARM	2G Enterprises cryogenic magnetometer (2G-755-SRM)	10 steps: 0, 5, 10, 20, 30, 40, 50, 65, 80 and 100 mT	46 samples (6 cm^3)
Imparting of a saturation isothermal remanent magnetization (SIRM)	2G Enterprises 660 pulse Magnetizer (max. amplitude 2.7T)	Produced along positive *z*-axis peak field of 1.0, 1.5 T and 2.0 T	46 samples (6 cm^3)
Measurement of SIRM	Molyneux Minispin Fluxgate magnetometer (Minispin)		46 samples (6 cm^3)
Measurement of hysteresis parameters M_S, M_{SR}, B_C and B_{CR}	Micromag Alternating Gradient Magnetometer (Princeton Measurements Corporation)	Max. field 500 mT	104 pellets weight: 3–60 mg
Imparting of complete IRM-acquisition curves	MicroMag	61 logarithmic equidistant steps from 0.2 to 2.0 T	92 pellets

several minutes until a homogenous colouring was observed. They were then poured into standard palaeomagnetic plastic boxes with a volume of 6 cm^3 (2.0 × 2.0 × 1.5 cm). Forty-six samples were prepared with a haematite concentration ranging between 0 and 100 wt-% of the total magnetic fraction. Small (3–60 mg) pellets were also prepared for measurement with a Princeton Measurements Corporation Alternating Gradient Magnetometer (AGM). For every defined magnetite/haematite ratio, three pellets were analysed to monitor for sample inhomogeneity. For comparison, four larger samples were prepared by mixing either haematite or magnetite, together with small quantities of Al_2O_3 powder and glue in 6 cm^3 plastic boxes. The remaining volume was filled with non-magnetic plastic foam. The 'natural' remanent magnetization (J_{NRM}), acquired during hardening of the resin and the glue, was measured with a cryogenic magnetometer (2G-Enterprises Model 755SRM), and then demagnetized at 50 and 100 mT to minimize its contribution to the subsequently imparted artificial magnetizations. All samples were then subjected to a set of standard measurements using equipment and parameter settings as listed in Table 1. In general, the field settings chosen for the laboratory induced magnetizations correspond to those typically selected for sediment samples containing mainly (Ti-) magnetite. This was done to enable comparison with results from rock magnetic studies on natural sediments. High-temperature saturation magnetization measurements were made in an argon atmosphere for four resin-free samples containing variable amounts of magnetite, hematite and Al_2O_3 powder. Measurements were performed with a variable field translation balance (VFTB) with an applied field of 550 mT and at temperatures of up to 700 °C, with heating/cooling rates of 40 °C min^{-1}. S-ratios were calculated for different magnetizing fields (SIRM) and backfields (IRM_R), following the procedures used by both Bloemendal *et al.* (1988) {S-ratio = 0.5 × [1 – (IRM_R/SIRM)]} and King & Channell zeichen (1991) [S-ratio = –IRM_R/SIRM]. The hard IRM (HIRM) was calculated following King & Channell (1991) [HIRM = 0.5 × (SIRM – IRM_R)]. Hysteresis parameters were calculated after paramagnetic slope correction. The ARM intensity, J_{ARM}, was divided by the strength of the applied steady field (50 μT), and is expressed as anhysteretic susceptibility, κ_{ARM}.

RESULTS AND DISCUSSION

High-temperature saturation magnetization measurements of a 100 wt-% magnetite sample reveal that maghaemite has formed by low-temperature oxidation during the 7 yr of storage of the magnetite powder (Fig. 1a). The maghaemite starts to invert to haematite at around 350 °C, which lies within the wide range (250–900 °C) reported in the literature (Dunlop & Özdemir 1997, and references therein). Based on the observed difference in magnetization between the heating and the cooling curve at 70 °C, about 20 per cent of the saturation magnetization is carried by maghaemite (Fig. 1a). The curvature of the heating and cooling curves, and a Curie temperature of 680 °C obtained from the sample containing 100 wt-% haematite powder (Fig. 1d) correspond to those expected for non-saturated, pure and 'defect-pure' haematite with a paramagnetic contribution of around 30 per cent to the initial total magnetization (Boer & Dekkers 1998). There is also evidence for the presence of magnetite and maghaemite in the haematite samples. The latter is again identified by the inversion temperature of 350 °C, with a small loss of magnetization at 580 °C indicating the presence of magnetite (Fig. 1d). The purity of the Fe_2O_3 powder is 99.945 per cent, so it can be assumed that up to 0.055 per cent of the magnetic fraction was originally composed of magnetite, which would contribute around 10 per cent of the total magnetization, based on a saturation magnetization (M_S) of 480 and 2.5 kAm^{-1} for magnetite and haematite, respectively (Thompson & Oldfield 1986). Magnetic parameters for maghaemite are similar to those for magnetite, so we do not treat the maghaemite separately, but hereafter refer to the ferrimagnetic component as 'magnetite'. The results of high temperature runs of magnetite/haematite mixtures, with haematite carrying about 5 and 30 per cent of the magnetization, respectively, are presented in Figs 1(b) and (c) .

The dependence of mass-normalized magnetic concentration-related parameters, κ_{ARM}, low-field magnetic (bulk) susceptibility (κ_{LF}) and IRM on haematite concentration is shown in Fig. 2 and Table 2. The M_S of the magnetite powder is 150 times higher than that of the haematite powder. That is distinctively lower than the value of 192 as given in the literature (Dunlop & Özdemir 1997), and must be attributed to the impurity in the studied haematite sample. Remarkably, there is no real difference between IRM acquired with fields of 1.0, 1.5 or 2.0 T (Fig. 2). A factor of around 450 is obtained for κ_{ARM} (Mt 100 wt-%)/κ_{ARM} (Ht 100 wt-%) because the haematite was not saturated during ARM aquisition. Dividing κ_{LF} measured for 100 wt-% magnetite by that for 100 wt-% haematite, the calculated factor of 670 is 30 per cent lower than literature values (Soffel 1991). This

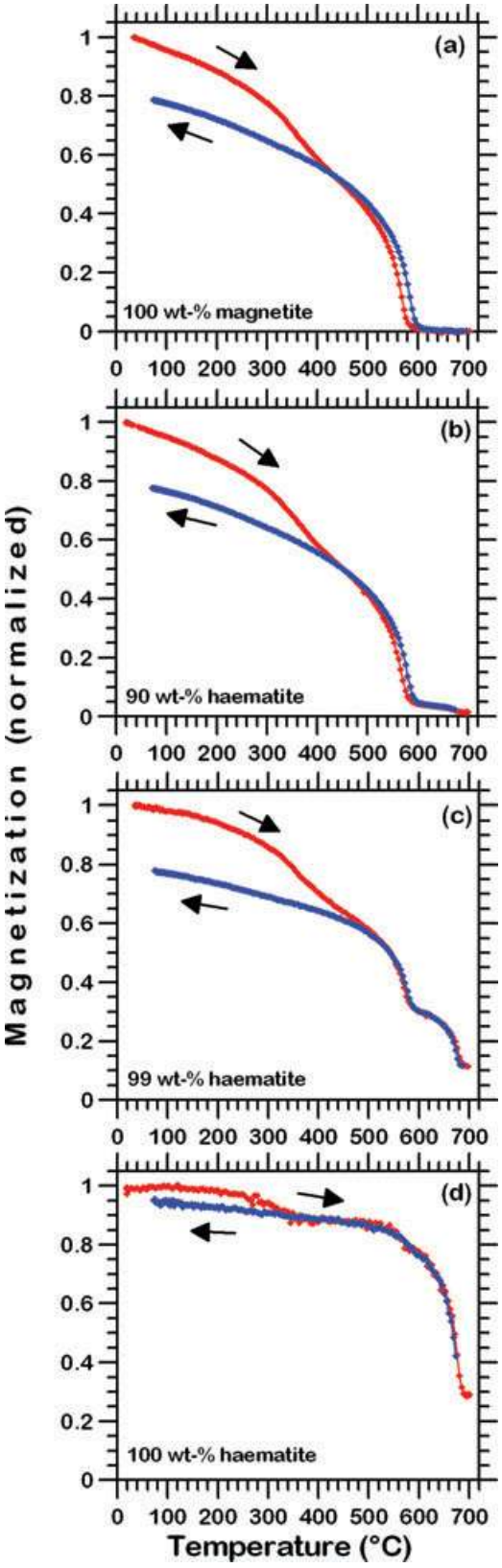

Figure 1. High-temperature measurements of the saturation magnetization for samples prepared with different magnetite/haematite ratios and Al_2O_3 as a non-magnetic matrix, measured with a variable field translation balance (VFTB). Red diamonds denote heating curves and blue diamonds denote cooling curves. Determinations were carried out on about 0.1–0.2 cm^3 of powder mixtures.

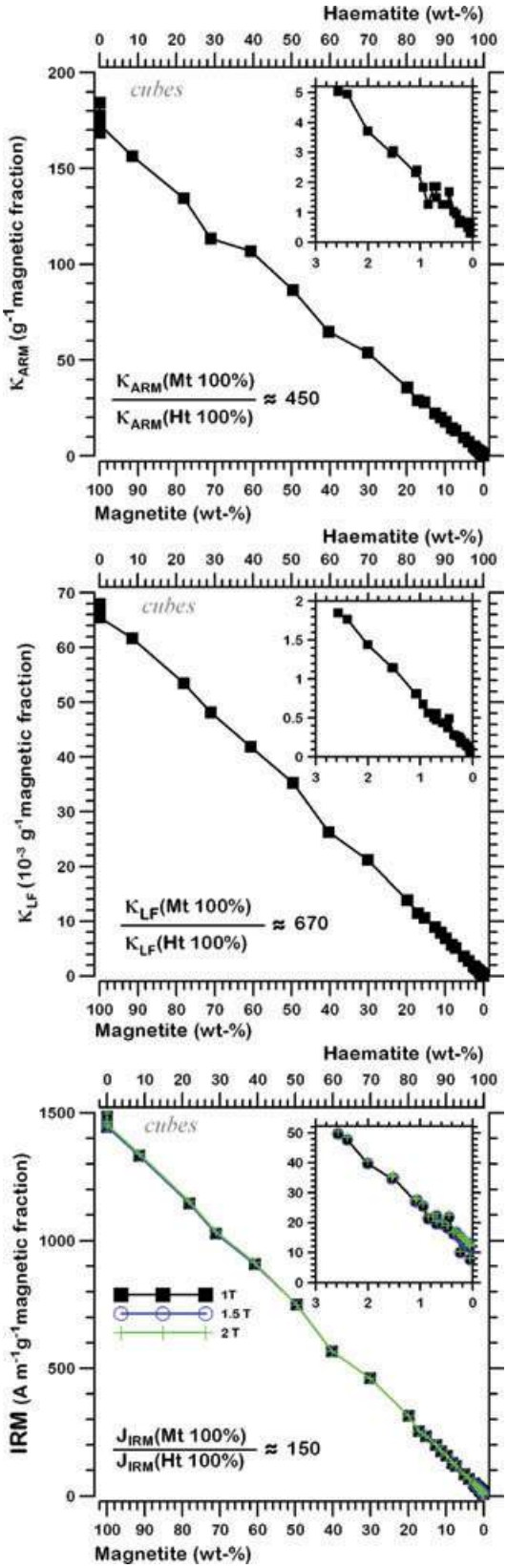

Figure 2. Variations of mass-normalized concentration dependent magnetic parameters for variable mixtures of haematite-magnetite: susceptibility of the anhysteretic remanent magnetization (κ_{ARM}), low-field magnetic susceptibility (κ_{LF}) and isothermal remanent magnetization (IRM) are plotted. Determinations were carried out on 6 cm^3 samples. The insets are enlargements of the lower rigth end of the curves.

Table 2. Results of standard rock magnetic measurements for different magnetite/haematite mixing ratios.

Haematite (wt-%)	MDF_{ARM} (mT)	κ_{ARM} (g^{-1})	$IRM_{1.5T}$ (mA m-1 g^{-1})	κ_{LF} (g^{-1})
0	28.2	168.67	1467.01	67.98
0	28.8	177.87	1493.89	67.32
0	27.8	174.03	1452.98	66.86
0	28.4	172.88	1452.21	65.47
8.44 (8.44)	27.8	156.61	1339.20	61.68
21.87 (21.85)	27.8	134.65	1145.83	53.50
28.9 (28.89)	27.0	113.55	1034.01	48.18
39.3 (39.28)	28.3	106.90	914.12	41.92
50.35 (50.32)	27.9	86.61	750.73	35.26
59.73 (59.69)	27.8	64.72	567.41	26.28
69.9 (69.87)	28.5	53.92	462.40	21.21
80.15 (80.11)	28.1	35.74	314.96	13.90
82.88 (82.84)	28.8	29.12	254.97	11.47
84.67 (84.62)	29.3	28.08	236.59	10.62
87.35 (87.31)	28.5	22.35	201.77	8.97
88.8 (88.759	28.7	20.16	173.61	7.98
90.19 (90.14)	29.3	18.02	159.15	6.88
91.75 (91.7)	28.7	14.58	129.96	5.75
92.72 (92.67)	29.4	13.26	118.96	5.13
94.92 (94.87)	30.0	9.69	86.50	3.65
96.16 (96.1)	29.9	7.41	69.31	2.79
97.48 (97.43)	30.7	5.03	50.31	1.85
97.65 (97.6)	31.9	4.95	48.10	1.77
98.05 (98.0)	30.0	3.71	40.16	1.45
98.5 (98.45)	30.5	2.98	35.24	1.15
98.54 (98.48)	30.8	3.07	35.50	1.15
98.96 (98.91)	33.5	2.32	27.68	0.81
98.98 (98.93)	34.1	2.42	27.88	0.82
99.1 (99.05)	30.0	1.85	26.36	0.68
99.2 (99.15)	28.5	1.28	22.04	0.57
99.3 (99.25)	38.1	1.86	21.99	0.51
99.35 (99.3)	44.6	1.86	20.17	0.48
99.48 (99.43)	34.8	1.28	20.05	0.45
99.57 (99.52)	39.4	1.27	18.85	0.38
99.69 (99.64)	39.4	1.04	16.78	0.29
99.75 (99.69)	42.5	0.95	17.35	0.28
99.8 (99.75)	34.8	0.64	15.87	0.25
99.83 (99.78)	39.8	0.68	15.34	0.22
99.87 (99.82)	49.1	0.68	14.73	0.18
99.9 (99.85)	#	#	14.41	0.18
99.93 (99.88)	#	#	13.96	0.15
99.96 (99.9)	48.7	0.49	13.69	0.14
99.99 (99.94)	77.6	0.69	12.58	0.10
100 (99.945)	85.0	0.59	12.48	0.10
100 (99.945)	#	#	12.41	0.10
100 (99.945)	67.6	0.41	12.44	0.10
100 (99.945)	58.5	0.32	8.09	0.07

Note: # no ARM-data available. κ_{ARM}, $IRM_{1.5T}$ and κ_{LF} are normalized for the mass of the total magnetic fraction. The numbers in brackets denote the haematite content after correction for a magnetite impurity. For detailed explanation, see text.

is probably because of magnetite contamination in the haematite powder, as discussed above. In order avoid this problem, the mass values of the haematite component in the samples were corrected, assuming that the known impurity of 0.055 wt-%, as given by the producer of the Fe_2O_3 powder, is all magnetite (Table 2).

Alternating field (AF) demagnetization of the ARM (6 cm^3 samples), IRM acquisition and hysteresis loops (pellet samples), for 10 selected mixtures are shown in Fig. 3. The most remarkable result of these analyses is that the haematite content must exceed 80 wt-% of the magnetic mineral fraction, that is ∼2 per cent of the total magnetization, before it becomes visible in the IRM acquisition curves (Fig. 3d). To obtain an IRM that is carried equally (50:50) by magnetite and haematite, 99.5 wt-% of the magnetic fraction must be composed of haematite (Fig. 3h).

ARM demagnetization and hysteresis loops are relatively unaffected by haematite admixtures with magnetite. The haematite content must climb above 90 wt-% to start to have a visible impact on results and the results are only markedly affected above 99 wt-% haematite (Fig. 3). This corresponds to the observations made using FORC-diagram (Muxworthy *et al*. 2005; Carvallo *et al*. 2006). Wasp-waisted loops, as described for samples with contributions from high- and low coercitivity minerals (Roberts *et al*. 1995; Tauxe *et al*. 1996), are only observed for mixtures containing ≥99.5 wt-% haematite (Figs 3h–j). This observation must be interpreted

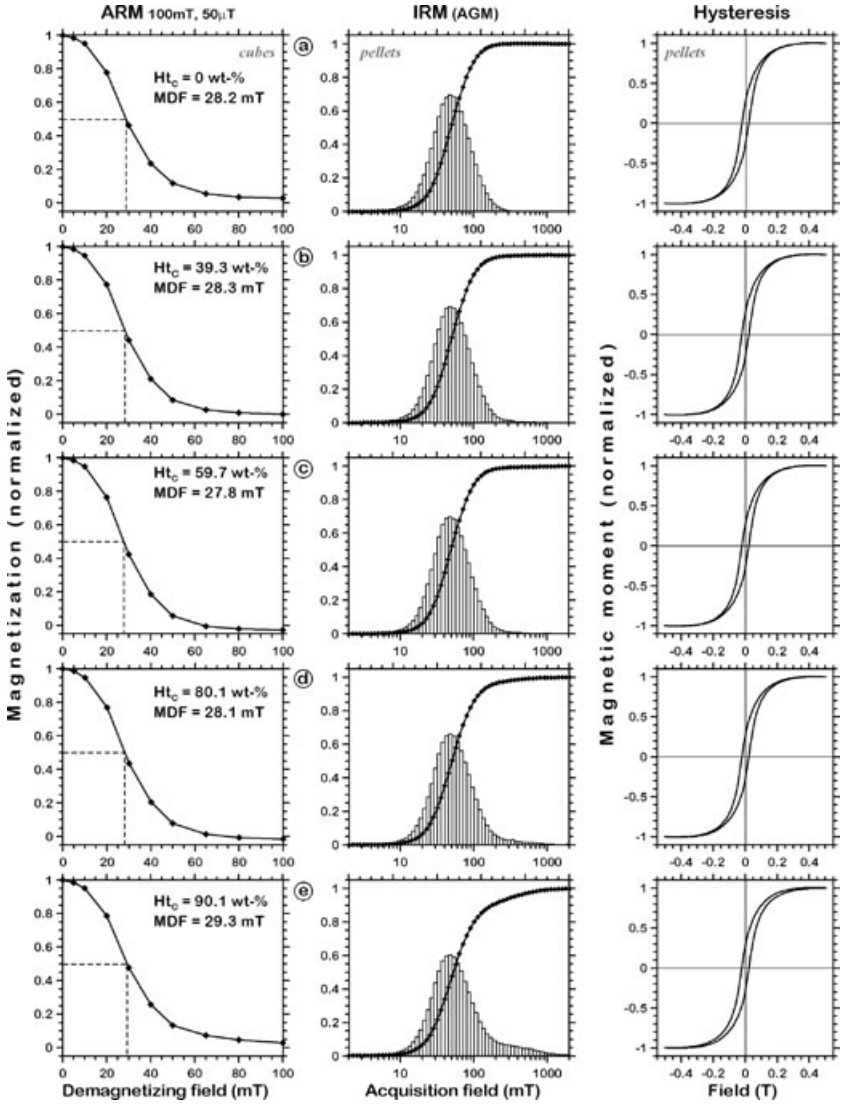

Figure 3. AF-demagnetization curves of the anhysteretic remanent magnetization (ARM, left-hand panels), acquisition curves and acquisition rates per field step (bars) of the isothermal remanent magnetization (IRM, middle panels), and hysteresis loops (right-hand panels) measured for ten samples with different magnetite/haematite ratios. The hysteresis loops are corrected for the paramagnetic slope. The ARM was measured on 6 cm^3 cubes, whereas the other parameters were determined on small (5–60 mg) pellets. Ht_C denotes the hematite content after correction for a magnetite impurity. For detailed explanation, see text.

with care, however because wasp-waistedness can occur when the components are not saturated.

The relationship between haematite content and the median destructive field of the ARM (MDF_{ARM}) is shown in Fig. 4. Samples containing only magnetite have a MDF_{ARM} of 28 mT (Figs 3 and 4, Table 2), which corresponds to the values measured for synthetic magnetite with a grain size of 2 μm (Maher 1988). For samples with >99 wt-% haematite, the MDF_{ARM} markedly increases with increasing haematite content. Two of the investigated 99.945 wt-% haematite samples have MDF_{ARM} values of 68 and 85 mT (Table 2). The MDF_{ARM} values are scattered for haematite contents >99 wt-% because haematite is far from saturated in the field used for ARM acquisition (Table 1).

Similar results were obtained when plotting the coercivity of remanence (B_{CR}) and coercive force (B_C), and the ratios of saturation remanence to saturation magnetization (M_{RS}/M_S) and B_{CR}/B_C versus haematite content (Fig. 5, Table 3). Again a marked increase is observed in these parameters when >92 wt-% of the magnetic fraction is haematite, except for the B_{CR}/B_C ratio which has a local maximum at haematite contents of 99–99.8 wt-% (Fig. 5). The mean B_{CR}/B_C value obtained for four 99.945 wt-% haematite samples is 1.42, which is distinctively lower than the value (1.62) obtained for the 100 wt-% magnetite samples. When plotting the M_{RS}/M_S versus B_{CR}/B_C (Day *et al.* 1977), the samples divide into two roughly linear trends, but with different gradients (Fig. 6). The reasons for these differences relates to the mixture of magnetic minerals with different coercitivities. Roberts *et al.* (1995) showed that in magnetic mixtures B_C is controlled by the magnetically soft component (magnetite) and B_{CR} by the magnetically hard component (haematite), which can result in wasp-waisted hysteresis loops if the two components have strongly contrasting coercitivities. Some of the data from Roberts *et al.* (1995) is shown in Fig. 6 for comparison. The relationship between the hard (soft) component and B_{CR} (B_C) changes when the magnetization carried by haematite exceeds the magnetite magnetization; at this point haematite also controls B_C. This change

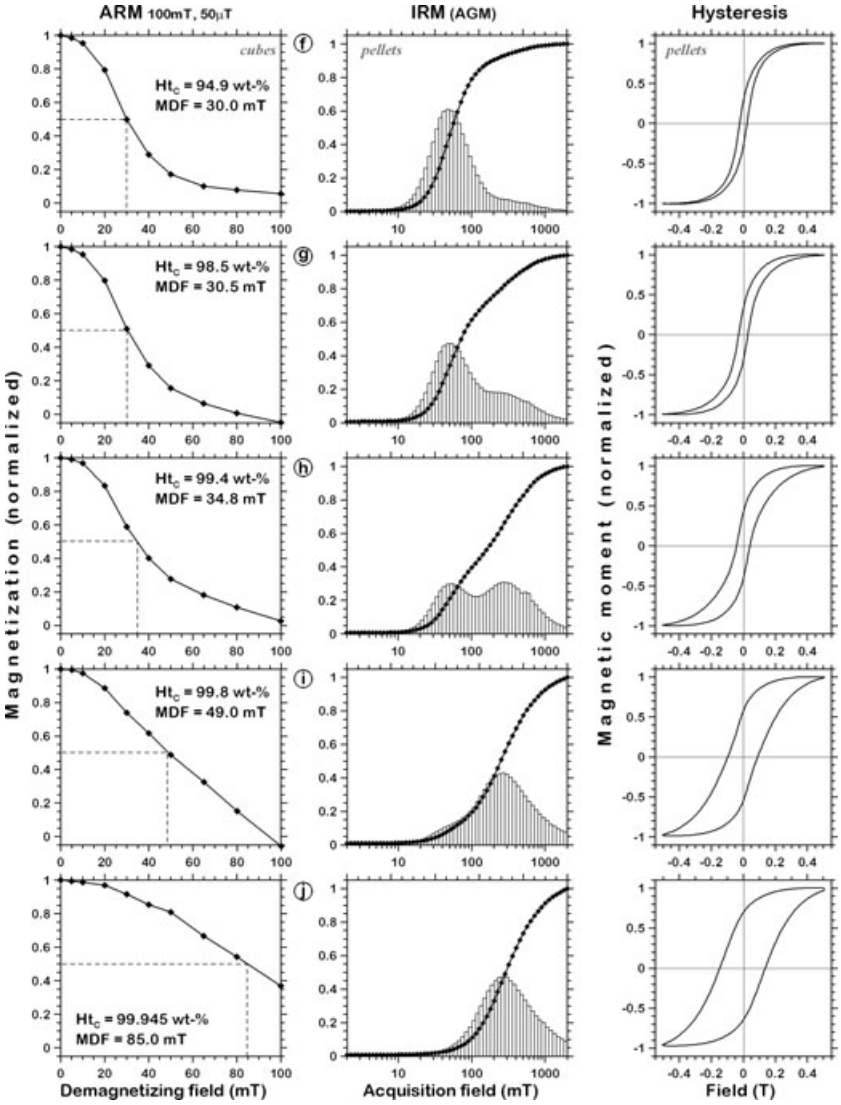

Figure 3. (*Continued*).

is also visible in Fig. 6, where B_C and B_{CR} are plotted versus M_{RS}/M_S. The slope of the linear distribution of B_C values abruptly decreases (on the basis of available data) for $B_C > 45$ mT, corresponding to a haematite concentration >99.5 wt-%, whereas the slope for B_{CR} undergoes two abrupt changes.

All M_{RS}, M_S, B_C and B_{CR} values determined from measurements with a maximum field of 0.5 T and those measured with a 2 T field increase with increasing maximum field, but to different extents. The increase in B_{CR} and B_C values varies between 5 and 20 per cent, causing non-systematic changes in the B_{CR}/B_C ratio (Fig. 7). In contrast, M_S and M_{RS} increase between 20 and 100 per cent and 10 and 80 per cent, respectively. The increase in M_{RS} for a given sample is constantly lower than for M_S, which results in a distinct shift to lower M_{RS}/M_S values when using a 2T maximum field (Fig. 7). The distribution pattern of the data remains the same, with a change in the trend at 99.5 wt-% haematite.

The widely applied parameter for estimating the relative concentration of haematite the S-ratio, using the different formulars of Bloemendal *et al.* (1988) and King & Channell (1991), is shown against haematite concentration in Figs 8(a) and (b), respectively. Different saturation fields and backfields, as typically used in different laboratories were used to calculate the S-ratios in order to obtain a wide range of data for comparison. As shown in Fig. 2, differences in IRM obtained with different peak fields (1.0, 1.5 and 2.0 T) can be ignored. Thus, the calculated S-ratios are mainly controlled by two parameters: haematite content and the applied backfield. Following the definition by Bloemendal *et al.* (1988), the lowest S-ratios with a mean value of 0.1 are obtained with a backfield of 0.1 T and a saturation field of 1 T for the four 99.945 wt-% haematite samples (Fig. 8). For a backfield of 0.3 T (saturation field 1.5 T), the mean S-ratio is 0.56 for the same samples. Grain size variations of the magnetite also affect the S-ratio, as indicated by the results of Bloemendal *et al.* (1992) in Fig. 8. It should be noted that the reference has been modified because the sample containing 100 per cent haematite was, for technical reasons, originally presented as 1 per cent magnetite (Bloemendal, personal commmunication, 2007). Using the formula of King & Channell (1991) similar results are obtained; the 99.945 wt-% haematite samples have the lowest values. The ideal S-ratio of 0 (–1) for pure haematite samples will not be achieved due to the low coercitive component of the haematite, as observed in the IRM acquisition curves (Figs 3h, i and j). Regardless, whether the applied backfield is 0.1, 0.2 or 0.3 T, the haematite content

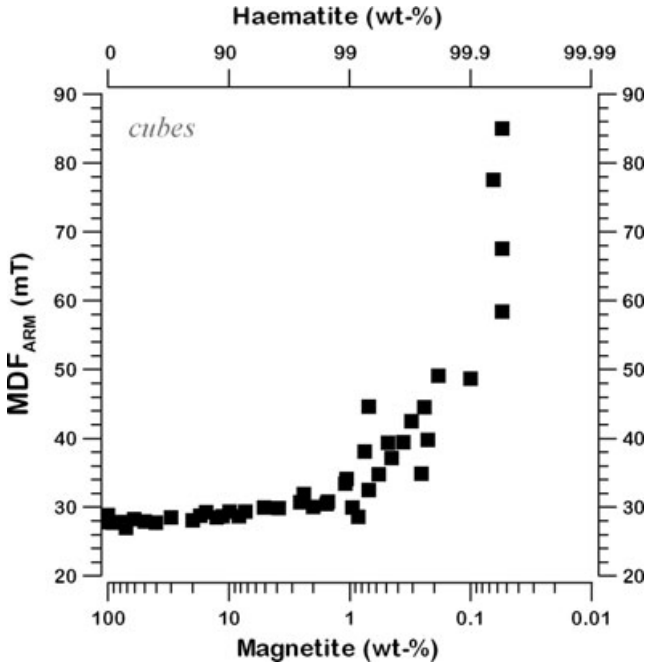

Figure 4. Relationship between median destructive field of the ARM (MDF_{ARM}) and haematite/magnetite content. Determinations were carried out on 6 cm^3 cubes.

must exceed 50 wt-% before it has a notable effect on the S-ratio (Fig. 8).

A second well known and widely used parameter for quantifying the contribution of high coercivity magnetic minerals is the HIRM. The advantage of this parameter is that it enables the calculation of the absolute concentration of haematite and/or goethite because, theoretically, the major difference in remanence between the SIRM and the backfield will be due to imperfect antiferromagnets such as goethite and haematite (Robinson 1986; Thompson & Oldfield 1986). The HIRM value like the S-ratio depends on the backfield-chosen (Fig. 9). The samples were weighed to maintain constant mass, therefore the HIRM values progressivly increase with haematite concentration. The biggest increase is from 0 to 90 wt-% haematite, with a more gentle increase from 90 to 99.945 wt-%. Problems for interpretation of the HIRM (and S-ratio), as summarized by Liu *et al.* (2007) are avoided in this study because we used the same technically produced Al-free haematite for the entire study. The major limitation of parameters such as HIRM and the S-ratio relate to the simplistic assumption that haematite starts to saturate at fields above 300 mT, which is obviously not true (Figs 3h–j). Use of a backfield of 200 mT for HIRM calculation unsurprisingly leads to higher absolute remanence values (Fig. 9), but this will partially involve contributions from magnetite as well as haematite. Additionally, Liu *et al.* (2002) demonstrated that the presence of a strong magnetic background (e.g. magnetite/maghaemite) can lead to high random and systematic errors in HIRM calculation that may distort the weak haematite signal. The values obtained for the 100 wt-% magnetite samples which should be zero, are probably affected by increasing inaccuracy of the Molspin spinner magnetometer with increasing attenuator scale, but it also reveals the problems pointed out by Liu *et al.* (2002).

Another motivation for this study was to estimate the influence of haematite content on some standard 'grain size' indicative

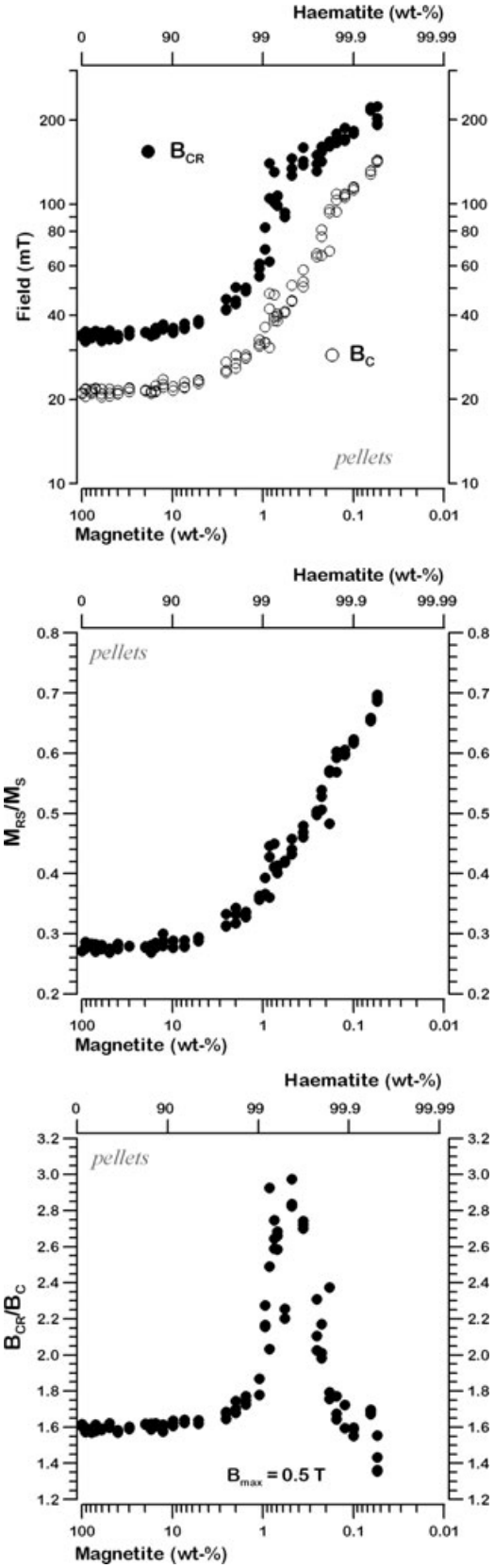

Figure 5. Relationship between the coercitivity of remanence (B_{CR}) and coercive force (B_C), the hysteresis ratios saturation remanent magnetization (M_{RS}) over saturation magnetization (M_S) and B_{CR}/B_C, and the haematite/magnetite content. Determinations were carried out on small (5–60 mg) pellets.

Table 3. Coercive force (B_C) and remanence coercitivity (B_{CR}) values for different magnetite/haematite mixing ratios.

Haematite$_C$ wt-%	B_{CR}(mT)	B_C(mT)
0	34.06	21.19
0	33.54	20.89
0	34.18	21.15
8.44	34.19	21.7
8.44	32.26	20.51
8.44	34.98	21.88
21.58	33.5	21.33
21.85	33.25	21.01
21.85	34.55	21.74
28.89	35.19	21.88
28.89	35.09	21.75
28.89	34.64	21.95
39.28	33.36	20.94
39.28	32.37	20.43
39.28	34.69	21.82
50.32	32.85	20.56
50.32	33.81	21.11
50.32	35.3	21.76
59.69	33.02	21.03
59.69	34.05	21.52
59.69	33	20.97
69.87	34.92	21.88
69.87	33.96	21.35
69.87	35.3	22.02
80.11	34.66	21.46
80.11	34.9	21.54
80.11	34.96	21.62
82.84	33.84	21.33
82.84	34.06	21.05
82.84	34.34	21.44
84.62	36	22.43
84.62	34.89	21.51
84.62	34.27	21.33
87.31	36.4	22.68
87.31	37.18	23.61
87.31	35.72	22.12
90.14	36.08	22.23
90.14	34.7	21.58
90.14	35.27	21.56
92.67	35.74	22.02
92.67	37.43	23.05
92.67	36.4	22.19
94.87	37.82	23.37
94.87	37.39	22.81
94.87	38.44	23.48
97.43	41.85	25.44
97.43	42.17	25.02
97.43	45.77	27.28
98.0	45.21	26.92
98.0	50.35	28.85
98.0	44.04	25.89
98.45	50.32	28.81
98.45	49.83	28.14
98.45	48.76	28.27
98.91	58.97	31.58
98.91	55.16	31.02
98.91	61.18	32.76
99.05	69.04	31.88
99.05	82.68	36.34
99.05	68.97	31.98
99.15	62.26	30.63
99.15	140.1	47.9
99.15	105	42.19
99.25	101.4	38.34
99.25	130.2	47.4
99.25	102	39.41
99.3	106.6	39.72
99.3	107.4	40.39
99.3	98.8	38.24
99.43	90.12	40.94
99.43	93.24	41.36
99.52	134.3	45.17
99.52	126.7	44.85
99.52	145.5	51.32
99.64	159.5	58.2
99.64	137.9	50.65
99.64	142.6	52.8
99.75	149.8	64.86
99.75	131.2	64.75
99.75	139.7	66.4
99.78	160.8	81.14
99.78	142.2	65.53
99.78	153.6	76.43
99.82	161.3	67.92
99.82	167.8	95.53
99.82	167.1	93.17
99.85	173.1	103.4
99.85	179.2	109
99.82	166.3	93.95
99.88	171.5	107.5
99.88	168.9	105.9
99.88	187.6	108.9
99.9	178.8	115.2
99.9	182.6	114.4
99.9	178.8	112.7
99.94	222.3	131.1
99.94	220.2	131.7
99.94	216.4	128.2
99.945	192.2	141.9
99.945	194.1	142.4
99.945	203.1	141.7
99.945	223.7	144.1

Note: Measurement was performed on small pellets with a MicroMag AGM. Haematite$_C$ denotes the hematite content after correction for impurity. For detailed explanation, see text.

parameter ratios. That is, how much will the presence of haematite bias interparametric ratios such as the anhysteretic susceptibility over (low-field) bulk magnetic susceptibility (κ_{ARM}/κ_{LF}), anhysteretic susceptibility over saturation magnetization (κ_{ARM}/SIRM), as well as saturation magnetization over bulk magnetic susceptibility (SIRM/κ_{LF})? These results are shown in Fig. 10 together with the base parameters $\kappa_{ARM,}$ κ_{LF} and SIRM. In general, the haematite content must exceed 90–95 wt-% of the magnetic fraction before a notable change is observed in all three parameters. This corresponds to the results of Bloemendal *et al.* (1992), who also stated that κ_{ARM}/κ_{LF} is relatively insensitive to increasing haematite contributions compared to magnetite grain size dependency (Fig. 10). Comparing the interparametric ratio curves with the single parameter curves, it is evident that changes in κ_{ARM}/SIRM and

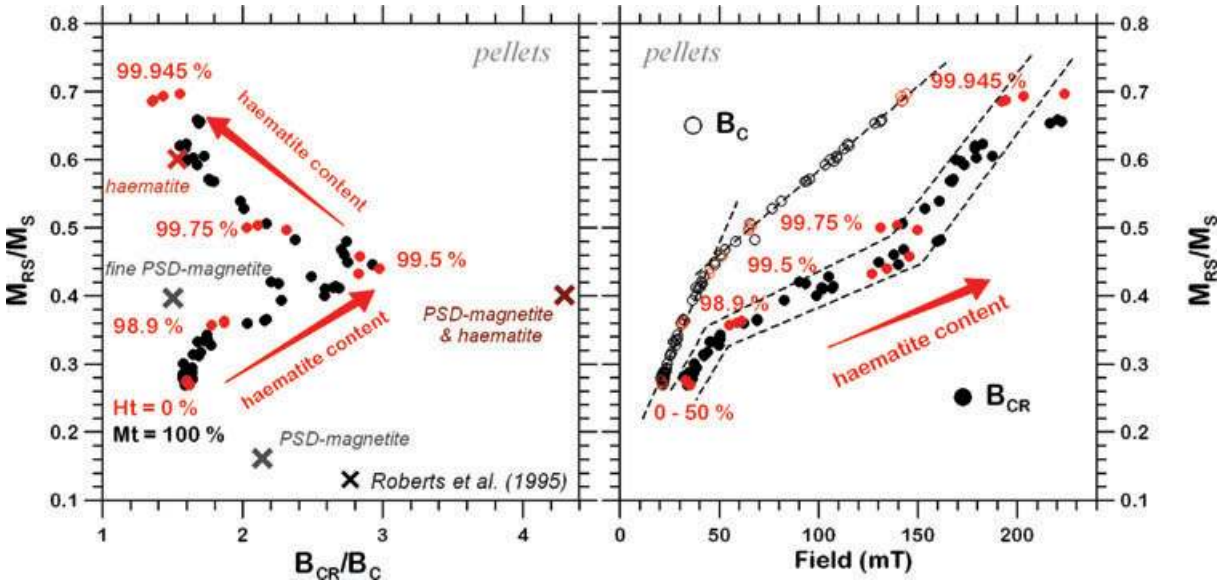

Figure 6. Bi-plots of M_{RS}/M_S versus B_{CR}/B_C (left-hand panel) and M_{RS}/M_S versus B_{CR} (closed circles) and B_C (open circles, right-hand panel). The numbers denote the content in wt-%, Ht= haematite, Mt= magnetite. The data points marked by coloured crosses are taken from Roberts *et al.* (1995). Red circles denote the samples for which the haematite content is given in the figure.

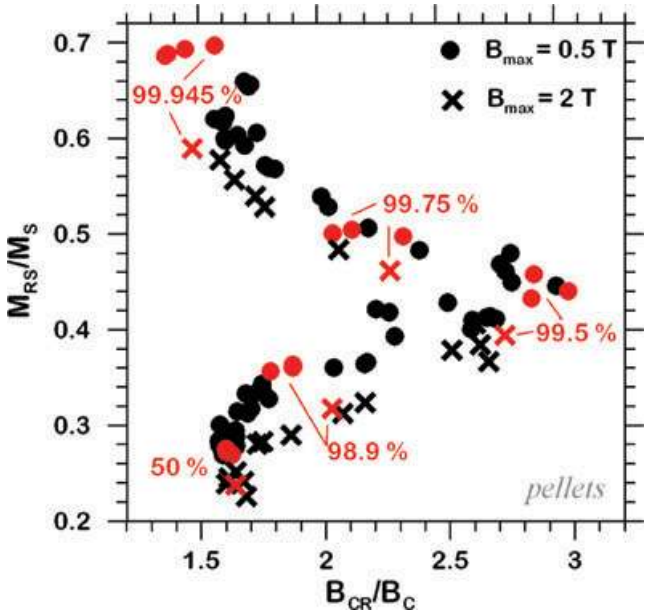

Figure 7. Comparison of M_{RS}/M_S and B_{CR}/B_C values in a Day-plot (Day *et al*. 1977). The corresponding hysteresis parameters were measured with different fields: dots: 0.5 T maximum field, crosses: 2 T maximum field. Data were obtained for samples with haematite contents between 99.1 and 100 wt-%. The red numbers denote the haematite content in wt-% of the samples marked in red.

$SIRM/\kappa_{LF}$ are essentially generated by a reduced decrease in SIRM for >99 wt-% haematite.

High values of $SIRM/\kappa_{LF}$ are not only indicative of haematite but also of greigite (Snowball & Thompson 1990; Roberts & Turner 1993; Roberts 1995; Dekkers & Schoonen 1996) and increases in greigite content are also associated with increases in κ_{ARM}/κ_{LF} ratios (Dekkers & Schoonen 1996; Frank *et al*. 2007; Ron *et al*. 2007). Several biplots of different magnetic parameters versus haematite content are therefore also used in Fig. 11 to provide a better overview of how variations in haematite content influences various rock magnetic parameters/parameter ratios. The main outcome is that variations in haematite content can be ignored when interpreting most of the rock magnetic parameters, especially κ_{ARM}/κ_{LF} and κ_{ARM}/SIRM, for samples with S-ratio > 0.88 (1.5 T saturation field, 0.3 T backfield), where haematite content is from 0 to 98 wt-% (cf. Fig. 8a). In samples with higher haematite contents the MDF_{ARM} and $SIRM/\kappa_{LF}$ values drastically increase. This parameter combination along with the S-Ratio is therefore ideal for identification of the presence of significant concentrations of haematite in natural samples. Additional confirmation of significant concentrations of haematite can be obtained using $B_{CR,}$ if measured, as shown in Fig. 12. Literature data for other minerals are taken from the compilation by Peters & Dekkers (2003). The data obtained from the haematite–magnetite mixtures in this study fit well within the gap between literature values for magnetite and haematite.

CONCLUSION

The intention of the present systematic study was to produce a standard set of rock magnetic parameters and parameter ratios from artificial samples with known magnetite/haematite ratios as a reference to aid interpretation of results from lacustrine and marine sediments. The simple approach used here demonstrates that the influence of haematite on most rock magnetic results can be widely ignored for haematite contents below 90–95 wt-% of the magnetic mineral fraction, when magnetite is also present. This is valid for the coercitivity-indicative parameters S-ratio, MDF_{ARM}, B_C and B_{CR}, which are more sensitive to haematite. However, ARM-based parameters suffer from data scatter due to incomplete saturation of haematite in standard ARM acquisition fields. To identify haematite in natural samples, it is useful to combine the S-ratio and $SIRM/\kappa_{LF}$ and, if available, $B_{CR.}$ The S-ratio clearly distinguishes haematite (low S-ratio) from greigite (high S-ratio), although we did not attempt to determine any information on how this magnetic parameter changes in a three-mineral-mixture. The S-ratio and the HIRM values presented display a range of values for samples containing

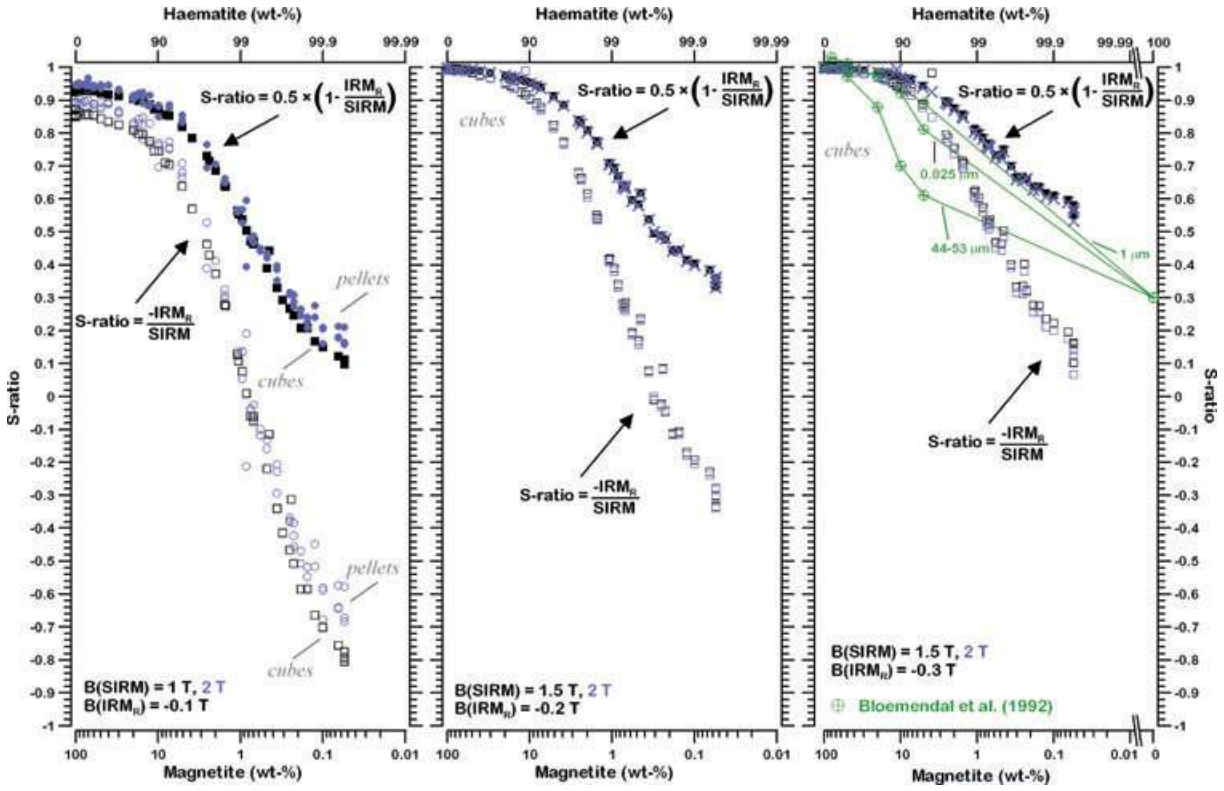

Figure 8. Dependence of S-ratios calculated with different formulas using different saturation and back-fields, and variable haematite/magnetite content. Closed symbols and crosses denote S-ratio = 0.5 × [1 –(IRM$_R$/SIRM)] (Bloemendal *et al.* 1988), open symbols denote S-ratio = –IRM$_R$/SIRM (King & Channell 1991). Determinations were carried out on 6 cm^3 cubes, except for the S-ratios with B(SIRM) = 2 T, B(SIRM$_R$) = 0.1 T. These measurements were performed on small pellets with the AGM. Results from Bloemendal *et al.* (1992) are also shown for different magnetite grain sizes (IRM was imparted with a saturation field of 1 T and a backfield of 0.3 T) (encircled green crosses).

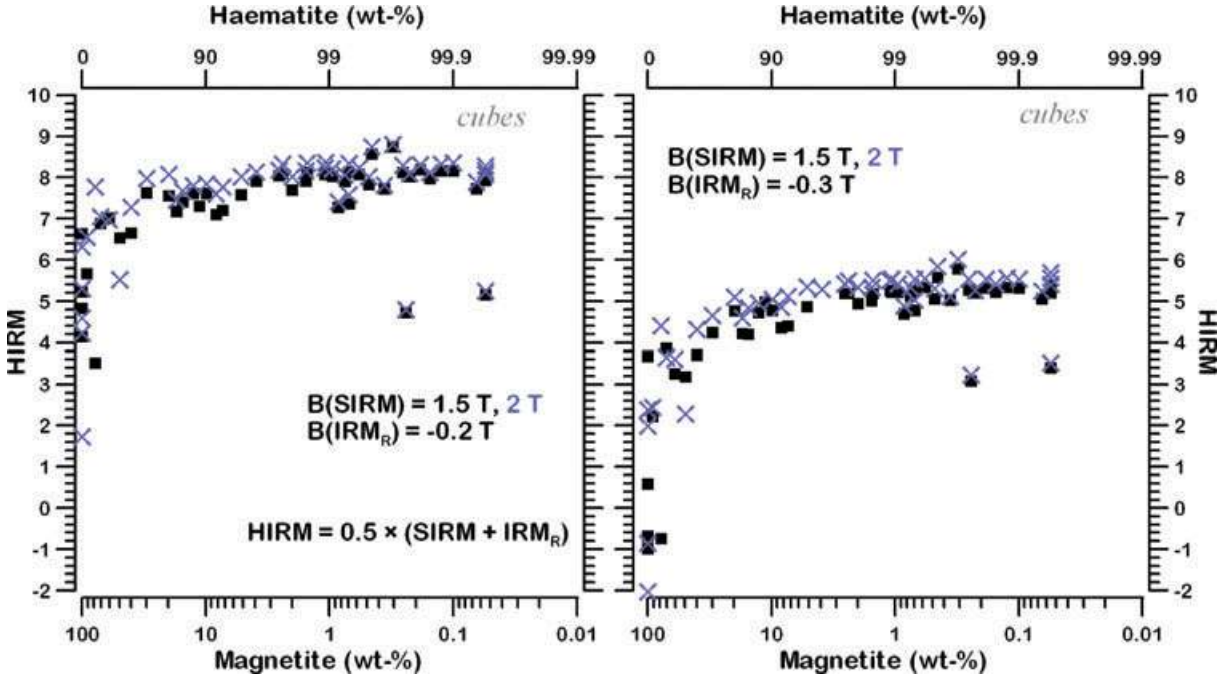

Figure 9. Dependence of HIRM calculated using different saturation and back-fields, and variable to haematite/magnetite content.

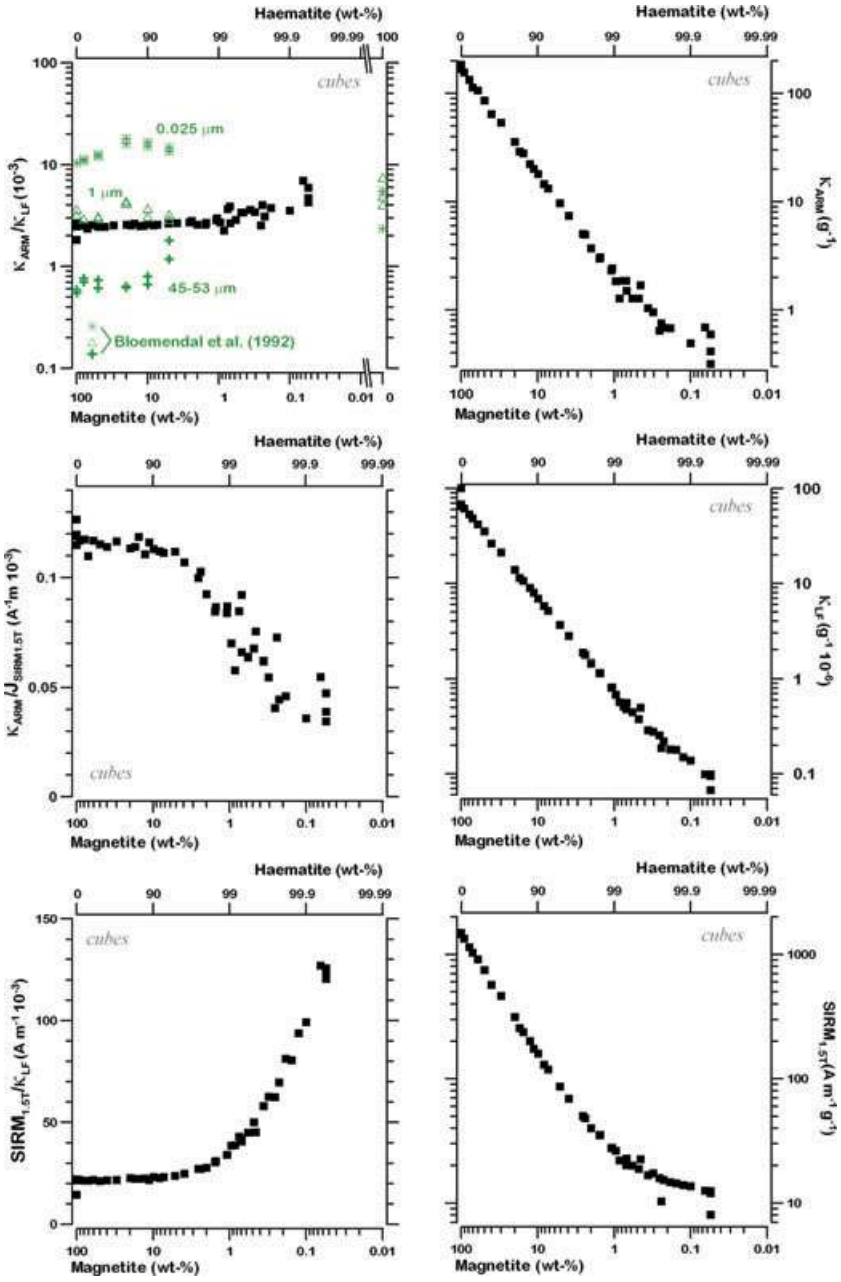

Figure 10. Dependence of magnetic 'grain size' indicative parameters κ_{ARM}/κ_{LF}, κ_{ARM}/SIRM and SIRM/κ_{LF} and the base parameters κ_{ARM}, κ_{LF} and SIRM on varying haematite/magnetite contents. Green symbols denote the results from Bloemendal *et al.* (1992) for different magnetite grain sizes; crosses: 45–53 μm, open triangles: 1 μm, asterisks: 0.025 μm.

only haematite or magnetite, which limits their use for quantitive estimation of haematite contributions. Much higher variability in these and the other parameters presented must therefore be expected when analysing mixtures with different magnetic grain sizes and/or cation substitution which affects the coercivity-dependent parameters. The absolute values presented here are therefore strictly only valid for the grain sizes and compositions of the magnetic minerals used in this study. However, the trends are likely to be similar for magnetite and haematite with other grain sizes and compositions. Further research should either concentrate on mixtures with different grain sizes, or new mixtures should be prepared with other common magnetic minerals such as goethite and/or greigite. The present study on mixtures of haematite and magnetite with constant grain sizes but variable concentration variations represents the 'tip of the iceberg' regarding the large number of possible relative combinations of magnetic minerals of various grain sizes to the magnetization of natural samples.

ACKNOWLEDGMENTS

G. Arnold, M. Köhler and S. Gehrmann are acknowledged for help during sample preparation. This manuscript was highly improved by the critical comments of M. Jackson and A. P. Roberts. This study was funded by the German Research Foundation (DFG), grant Fr1672/1-2.

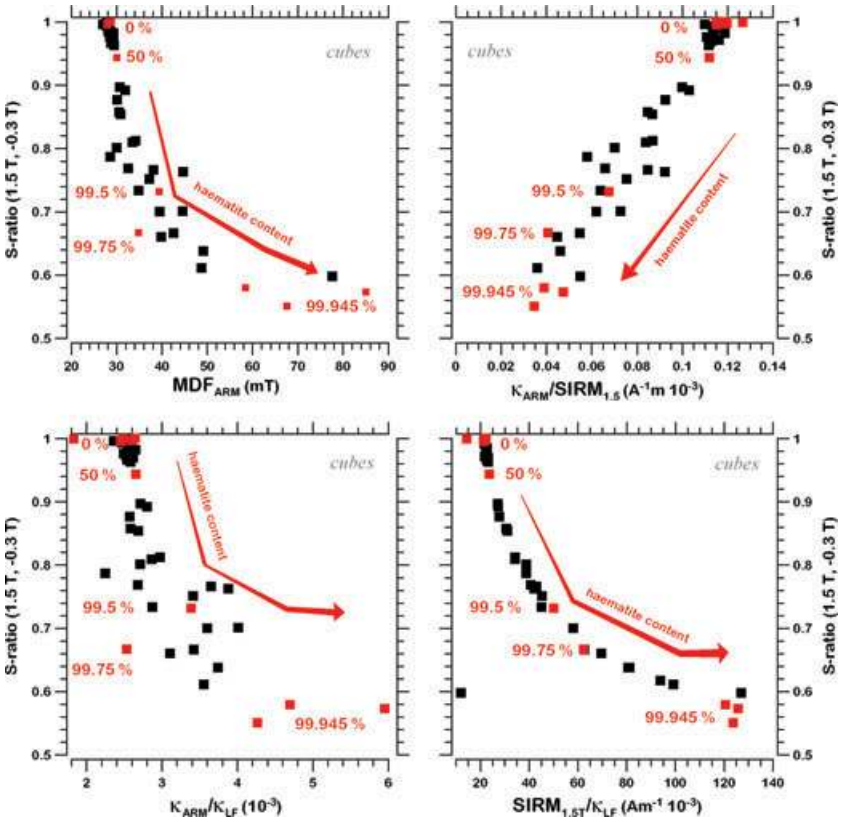

Figure 11. Bi-plots of different rock magnetic parameters and interparametre ratios illustrating the influence of variable haematite content. Numbers denote the haematite content of the samples in wt-% (red text).

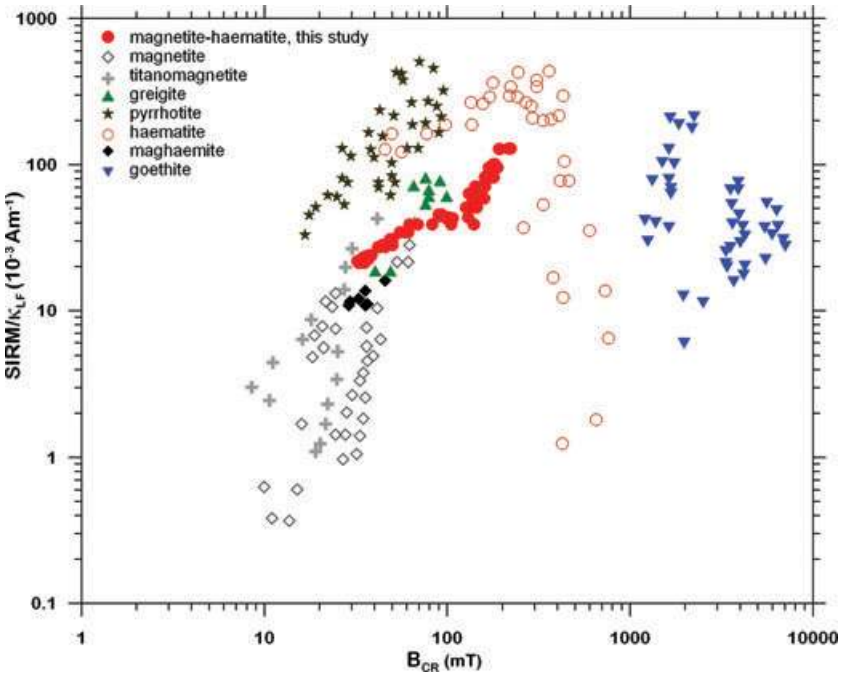

Figure 12. Bi-plots of SIRM/κ_{LF} versus B_{CR} for comparison of our haematite/magnetite mixtures with data from the literature for different magnetic minerals as compiled by Peters & Dekkers (2003).

REFERENCES

Bloemendal, J., Lamb, B. & King, J., 1988. Paleoenvironmental implications of rock-magnetic properties of late Quaternary sediment cores from the eastern Equatorial Atlantic, *Paleoceanography,* **3,** 61–87.

Bloemendal, J., King, J.W., Hall, F.R. & Doh, S.-J., 1992. Rock magnetism of late Neogene and Pleistocene deep-sea sediments: relationship to sediment source, diagenetic processes, and sediment lithology, *J. geophys. Res.,* **97,** 4361–4375.

Carter-Stiglitz, B., Moskowitz, B. & Jackson, M., 2001. Unmixing magnetic assemblages and the magnetic behavior of bimodal mixtures, *J. geophys. Res.,* **106,** 26 397–26 411.

Carvallo, C., Muxworthy, A.R. & Dunlop, D.J., 2006. First-order reversal curve (FORC) diagrams of magnetic mixtures: micromagnetic models and measurements, *Phys. Earth planet. Inter.,* **154,** 308–322.

Dankers, P., 1981. Relationship between median destructive field and remanent coercive forces for dispersed natural magnetite, titanomagnetite and haematite, *Geophys. J. R. Astron. Soc.,* **64,** 447–461.

Day, R., Fuller, M. & Schmidt, V.A., 1977. Hysteresis properties of titanomagnetites: grain size and compositional dependence, *Phys. Earth. planet. Inter.,* **13,** 260–267.

De Boer, C.B. & Dekkers, M.J., 1998. Thermomagnetic behaviour of hematite and goethite as a function of grain size in various non-saturating magnetic fields, *Geophys. J. Int.,* **133,** 541–552.

Dekkers, M.J. & Linsen, J.H., 1989. Rockmagnetic properties of fine-grained natural low-temperature haematite with reference to remanence acquisition mechanism in red beds, *Geophys. J. Int.,* **99,** 1–18.

Dekkers, M.J. & Schoonen, M.A.A., 1996. Magnetic properties of hydrothermally synthesized greigite (Fe_3S_4) – I. Rock magnetic parameters at room temperature, *Geophys. J. Int.,* **126,** 360–368.

Demory, F., Oberhänsli, H., Nowaczyk, N.R., Gottschalk, M., Wirth, R. & Naumann, R., 2005. Detrital input and early diagenesis in sediments from Lake Baikal revealed by rock magnetism, *Global planet. Change,* **46,** 145–166.

Dunlop, D.J. & Özdemir, Ö., 1997. *Rock Magnetism — Fundamentals and frontiers.* Cambridge Studies in Magnetism, 3. Cambridge University Press, Cambridge, 573 pp.

Frank, U., Nowaczyk, N.R. & Negendank J.F.W., 2007. Rock magnetism of greigite bearing sediments from the Dead Sea, Israel, *Geophys. J. Int.,* **168,** 921–934.

Geiss, C.E., Umbanhowar, C.E., Camill, P. & Banerjee, S.K., 2003. Sediment magnetic properties reveal Holocene climate change along the Minnesota prairie-forest ecotone, *J. Paleolim.,* **30,** 151–166.

Inoue, S., Hayashida, A., Kato, M., Fukusawa, H. & Yasuda, Y., 2004. Environmental magnetism of brackish-water sediments from Lake Tougou-ike on the Japan Sea coast, *Quat. Int.,* **123–125,** 35–41.

King, J.W. & Channell, J.E.T., 1991. Sedimentary magnetism, environmental magnetism and magnetostratigraphy, *Rev. Geophys.,* **29**(Suppl), 358–370.

Kumar, A.A., Rao, V.P., Patil, S.K., Kessarkar, P.M. & Thamban, M., 2005. Rock magnetic records of the sediments of the eastern Arabian Sea: evidence for late Quaternary climate change, *Mar. Geol.,* **220,** 59–82.

Larrasoaña, J.C., Roberts, A.P., Rohling, J., Winklhofer, M. & Wehausen, R., 2003. Three million years of monsoon variability over the northern Sahara, *Clim. Dyn.,* **21,** 689–698.

Lees, J.A., 1997. Mineral magnetic properties of mixtures of environmental and synthetic materials: linear additivity and interaction effects, *Geophys. J. Int.,* **131,** 335–346.

Liu, J., Zhu, R. & Li, G., 2003. Rock magnetic properties of the fine-grained sediment on the outer shelf of the East China Sea: implications for provenance, *Mar. Geol.,* **193,** 195–206.

Liu, Q., Banerjee, S.K., Jackson, M.J., Zhu, R. & Pan, Y., 2002. A new method in mineral magnetism for the separating of weak antiferromagnetic signal from a strong ferrimagnetic background, *Geophys. Res. Lett.,* **29,** doi:10.1029/2002GL014699.

Liu, Q., Roberts, A.P., Torrent, J., Horng, C.-S. & Larrasoaña, J.C., 2007. What do the HIRM and S-ratio really measure in environmental magnetism? *Geochem. Geophys. Geosyst.,* **8,** Q09011, doi:10.1029/2007GC001717.

Maher, B.A., 1988. Magnetic properties of some synthetic sub-micron magnetites, *Geophys. J.,* **94,** 83–96.

Muxworthy, A.R., King, J.G. & Heslop, D., 2005. Assessing the ability of first-order reversal curve (FORC) diagrams to unravel complex magnetic signals, *J. geophys. Res.,* **110,** B01105, doi:10.1029/2004JB003195.

Peters, C. & Dekkers, M.J., 2003. Selected room temperature magnetic parameters as a function of mineralogy, concentration and grain size, *Phys. Chem. Earth,* **28,** 659–667.

Roberts, A.P., 1995. Magnetic properties of sedimentary greigite (Fe_3S_4), *Earth planet. Sci. Lett.,* **134,** 227–236.

Roberts, A.P. & Turner, G.M., 1993. Diagenetic formation of ferrimagnetic iron sulphide minerals in rapidly deposited marine sediments, South Island, New Zealand, *Earth planet Sci. Lett.,* **115,** 257–273.

Roberts, A.P., Cui, Y. & Verosub, K.L., 1995. Wasp-waisted hysteresis loops: mineral magnetic characteristics and discrimination of components in mixed magnetic systems, *J. geophys. Res.,* **100,** 17909–17924.

Roberts, A.P., Liu, Q., Rowan, C.J., Chang, L., Carvallo, C., Torrent, J. & Horng, C.-S., 2006. Characterization of haematite (α-Fe_2O_3), goethite (α-FeOOH), greigite (Fe_3S_4), and pyrrhotite (Fe_7S_8) using first- order reversal curve diagramms, *J. geophys. Res.,* **111,** B12S35, doi,10.1029/2006JB004715.

Robinson, S.G., 1986. The late Pleistocene paleoclimatic record of North Atlantic deep-sea sediments revealed by mineral-magnetic measurements, *Phys. Earth planet. Inter.,* **42,** 22–47.

Ron, H., Nowaczyk, N.R., Frank, U., Schwab, M.J., Naumann, R., Striewski, B. & Agnon. A., 2007. Gregite detected as dominating remanence carrier in Late Pleistocene sediments, Lisan Formation, Lake Kinneret (Sea of Galilee), *Israel. Geophys. J. Int.,* **170,** 171–131.

Soffel, H.C., 1991. *Paläomagnetismus und Archäomagnetismus*. Springer Verlag, Berlin, Heidelberg, New York, 276 pp.

Snowball, I. & Thompson, R., 1990. A stable chemical remanence in Holocene sediments, *J. geophys. Res.,* **95,** 4471–4479.

Tauxe, L., Mullender, T.A.T. & Pick, T., 1996. Potbellies, wasp-waists, and superparamagnetism in magnetic hysteresis, *J. geophys. Res.,* **101,** 571–583.

Thompson, R. & Oldfield, F., 1986. *Environmental Magnetism*. Allen and Unwin, London, 227 pp.

Wang, H., Liu, H., Liu, Y. & Cui, H., 2004. Mineral magnetism of lacustrine sediments and Holocene paleoenvironmental changes in Dali Nor area, southeast Inner Mongolia Plateau, China, *Palaeogeogr. Paleoclimatol. Paleosyst.,* **208,** 175–193.